55-20
N96-70526
5943
P-14

ION THRUSTER DIAGNOSTICS

W. M. Ruyten*, V. J. Friedly**, X. Peng**, J. A. Celenza†
University of Tennessee-Calspan
Center for Space Transportation and Applied Research
Tullahoma, Tennessee 37388-8897

and

D. Keefer‡
Center for Laser Applications
University of Tennessee Space Institute
Tullahoma, Tennessee 37388-8897

Abstract

We report the results of spectroscopic investigations of beam-plasma interactions in the plume from a 3 cm ion source operated on argon. Ion-electron, ion-neutral, and electron-neutral scattering are identified by studying the dependence of neutral and ion emission intensities on chamber pressure and mass flow rate, and by analyzing the emission lineshapes at a non-orthogonal angle to the plume axis. Through the Doppler shift, we are able to separate contributions from fast beam ions and fast charge-exchange neutrals on the one hand, and of slow neutrals and slow ions on the other. We discuss the application of this new technique to the characterization of beam plasma interactions in the downstream region of ion thruster engines, and its potential for identifying the processes which lead to grid erosion.

1. Introduction

It has been suspected for a long time that one of the important mechanisms of accelerator grid erosion in ion thrusters is the production of charge-exchange ions in the downstream region of the plume. These ions are created at relatively small velocities. Thus they are accelerated back to the thruster grid, causing sputtering of the accelerator grid. We have performed extensive numerical studies of this process using particle-in-cell and Monte-Carlo techniques, and a number of papers on this work have been presented [1-8].

The numerical models are especially successful in calculating the pitted erosion patterns which develop during extended life testing of the grids. It appears that the models are also capable of yielding correct quantitative erosion rates. However, this requires knowledge of several experimental parameters which are not easily measured. One of these is the density distribution of neutral atoms near the grids, and the resulting production rate of charge-exchange ions as a function of position. Direct-Simulation-Monte-Carlo calculations are in progress to model the neutral efflux from the thruster in detail.

Most recently, it has been called into question whether the production of charge-exchange ions, by itself, can account for the observed impingement currents in ground tests [9]. It appears that even an ionization level as low as 0.01 percent of the background gas surrounding the thruster may be sufficient to provide the balance of the ion current on the accelerator grids, after charge-exchange is accounted for [8]. To model this extraction of ions from the plasma surrounding the thruster, it is necessary to know such properties as ion and electron temperatures, and the location and spatial extent of the plasma sheath which separates the thruster from its surroundings.

A standard technique for analyzing the above processes is through the use of electrical probes [10-13], and we

This work was supported jointly by Boeing Defense & Space Group of Seattle, Washington, and by the Center for Space Transportation and Applied Research.

* Principal Investigator; Calspan, Senior Engineer
** Research Engineer
† Graduate Student
‡ UTSI/CLA, B. H. Goethert Professor of ES&M

have reported the results of such measurements [14]. Here we investigate an alternative technique, based on spectroscopic measurements of line emissions from the ion plume. Similar types of optical studies have been performed previously [13,15-16]. However, an important innovation of our work is the use of a spectrometer with sufficient resolution (better than 0.1 Å fwhm) to study the Doppler shapes of the emission lines at a nonorthogonal observation angle to the plume axis.

All experiments were performed on the plume from a 3 cm ion source, operated on argon. We show that the production of charge-exchange neutral atoms can be identified unambiguously from the emission lineshapes. We are also able to identify the effects of ion-neutral scattering and electron excitation of beam ions, by studying the dependence of the emission intensities of both ion and neutral lines on source flow rate and facility background pressure. The results of the optical measurements appear to be consistent with the Langmuir probe studies, reported earlier [14].

We discuss the importance of the new spectroscopic technique to the characterization of plume plasma properties and beam-plasma interactions in ion thruster plumes. In particular, we identify possible ways in which the technique could be used to pinpoint the boundary conditions which are needed for a correct numerical simulation of the beam-plasma interactions and the resulting grid erosion in ion thrusters.

2. Experimental setup and procedure

Experimental measurements were performed on the plume from a commercial 3 cm ion source, operated on argon. A photograph of the source, Ion Tech model 3-1500-100, is shown in Fig. 1. A high-resolution spectrometer, a 1.25 m focal length SPEX with an 1800 gr/mm grating, was used to record line emissions from both neutral and singly ionized argon in the plume. Figure 2 shows a diagram of the optical setup. The ion source is mounted on a computer-controlled xyz stage inside the test facility. Plume emission is observed through a large optical access port.

Light from the plume is focused into the spectrometer by a large-aperture (f/6) Cassegrain telescope, mounted outside of the vacuum facility. The spectrometer was aligned either perpendicular to the plume, or at an angle of 71.4 degrees to the plume centerline (as shown in Fig. 2). A red-sensitized photo multiplier tube (PMT) served as the detector. The PMT signal was amplified and read out by the PC-based data acquisition system. Also, the signal was recorded simultaneously by a stripchart recorder.

For some of the experiments, the external neutralizer filament of the ion source was moved about 80 mm downstream from the grids. In this manner, it was possible to observe argon line emissions close to the source without picking up the strong continuum emission from the brightly glowing filament. Typical flow rates for the source were 4 to 12 sccm argon. Also, for a number of experiments the tank pressure was raised intentionally by flowing additional gas, also argon, into the facility through a bypass valve. Using a Balzers cryo pump, the resulting tank pressures were in the range 0.0013 to 0.04 Pa, or 1×10^{-5} to 3×10^{-4} Torr.

Discharge, beam, and accelerator voltages for the source were typically 50 V, 300 V to 1100 V, and -500 V, respectively. Typical beam currents were in the range 40 to 100 mA. These correspond to rather low propellant utilization efficiencies, especially for the higher flow rates. On the other hand, the large neutral loss from the source and the bypass flow into the chamber assured strong optical emissions from the plume, thereby simplifying the experimental measurements.

Horizontal slit widths of 10 to 100 microns were used on the spectrometer. These values correspond to spectral resolutions of 0.038 to 0.38 Å. Slit heights were 1 to 10 mm. An absolute calibration of the detection system was performed using a standard tungsten filament lamp. Measurements could be performed over the range 3300 to 8600 Å, with maximum sensitivity around 4500 Å. Wavelengths below 3300 Å are not transmitted by the optical access port of the vacuum chamber. Above 8600 Å, the quantum efficiency of the PMT falls off rapidly. Further details of the optical setup may be found in an accompanying paper on arcjet plume diagnostics [17].

3. Results of survey measurements

A broad survey scan of the plume revealed a rich spectrum of neutral (Ar I) and singly ionized argon (Ar II) emissions, superimposed on the continuum background from the filament. A small part of this spectrum is shown in Fig. 3. Using an atlas of argon lines [18], it was straightforward to identify the various lines. Moreover, it appears that all of the lines listed in the atlas were present in the plume spectrum.

It is important to note that the radiative lifetime for all observed lines is on the order of several nanoseconds. Thus, even for a 1000 eV ion, moving with a velocity of 70 km/sec, the "lifepath" of the excited state is less than 1 mm. This implies that any excited species created in the source have already decayed by the time they reach the observation region, some 20 to 100 mm downstream from

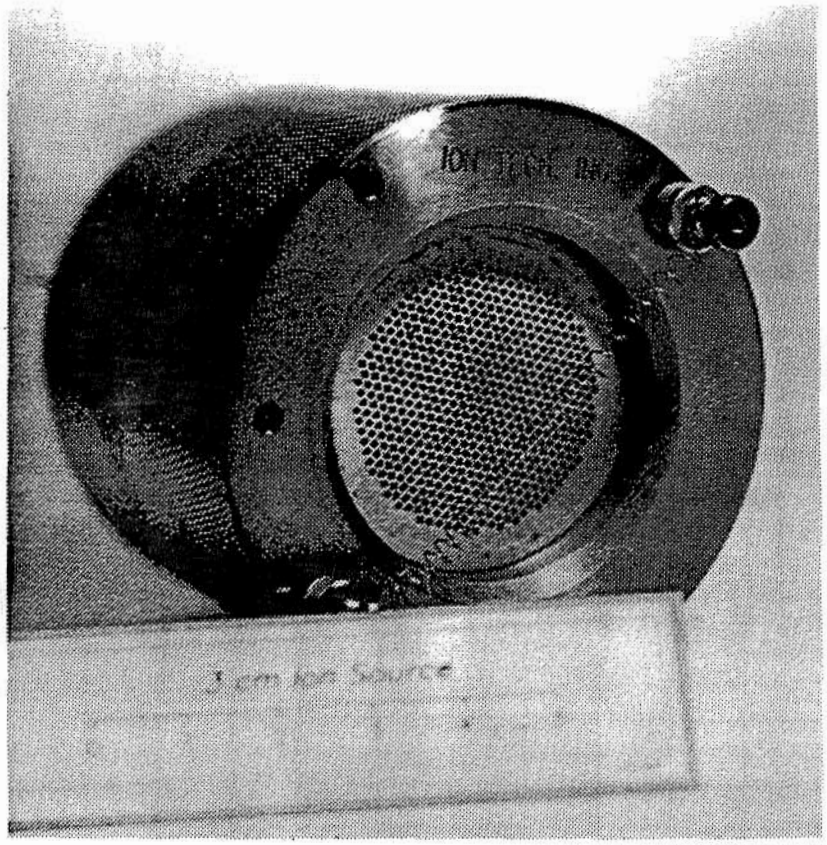

Figure 1: *Photograph of the 3 cm ion source.*

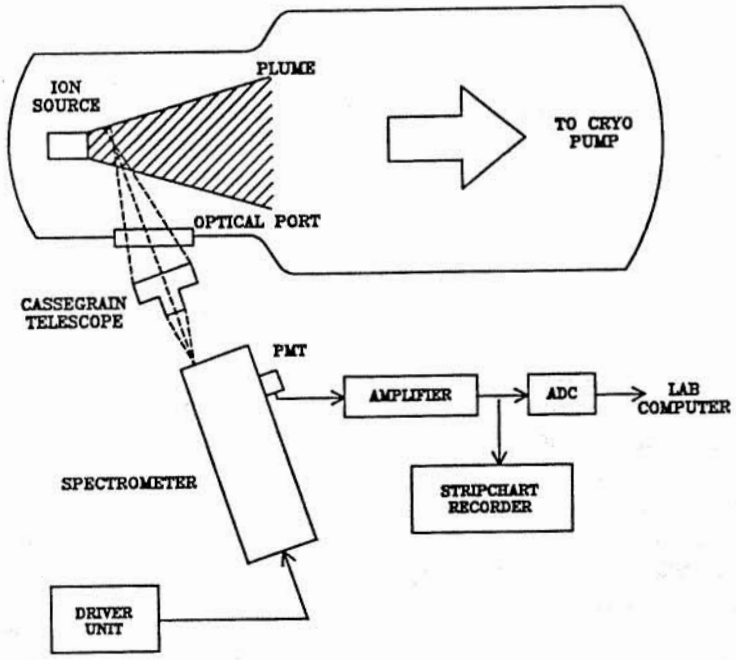

Figure 2: *Schematic of the optical setup.*

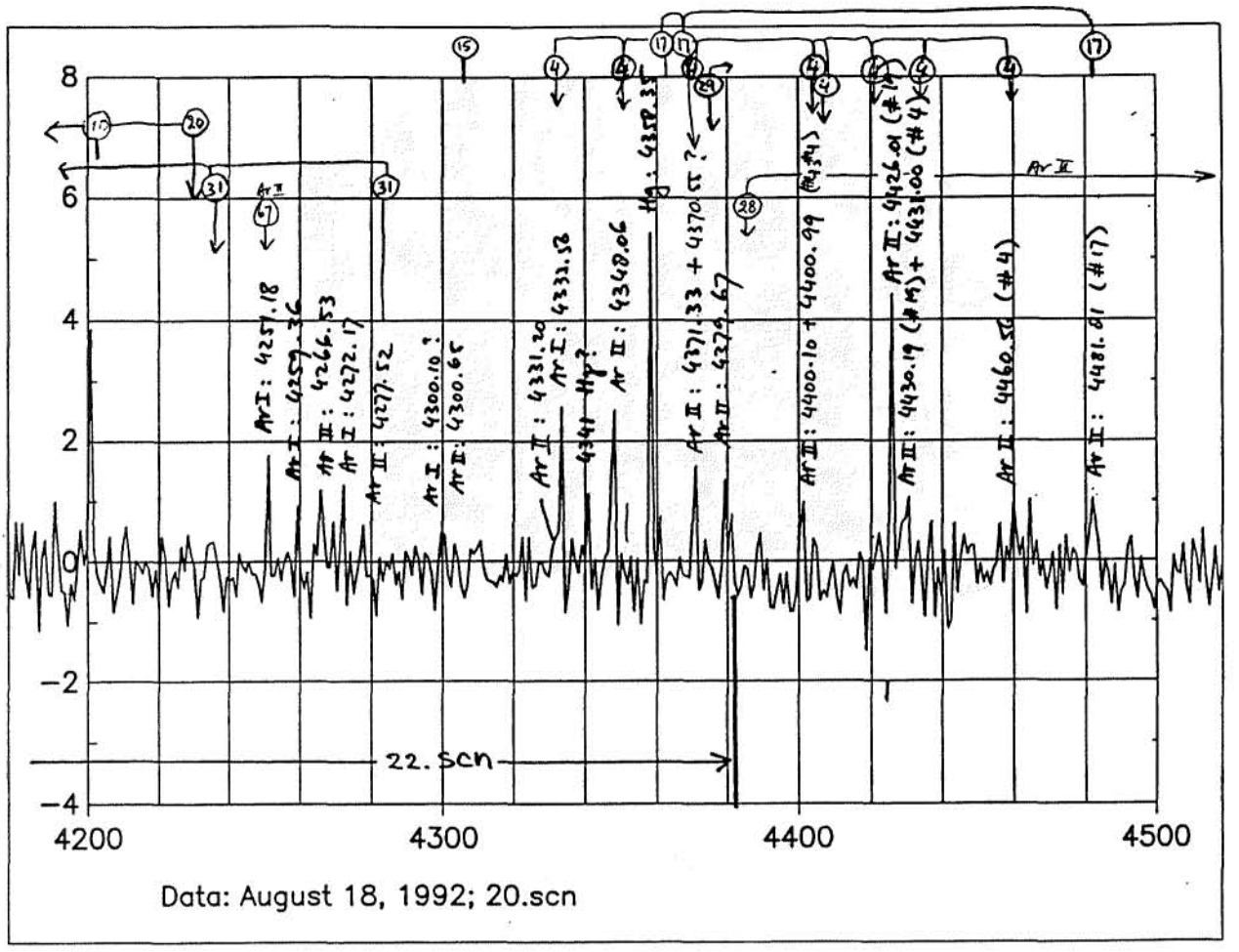

Figure 3: *Small section of a coarse survey scan, covering the range 4200 Å to 4500 Å of the argon plume spectrum. The baseline has been corrected for filament emission. Line designations and multiplet numbers from Ref. [18] are indicated, both for neutral (Ar I) and ion lines (Ar II). Many more lines can be identified by scanning smaller portions of the spectrum at slower rates.*

the accelerator grid. Thus all measured emissions must be the result of scattering and/or excitation processes which occur within the field of view of the optical system.

For a few selected spectral lines, the spatial variation of the plume emissions was established. Figure 4 shows the emission signals for a neutral line and a nearby ion line as a function of axial distance from the source. Clearly, the spatial variation of the two emission features is very similar. For reference, the emission from the filament is shown as well (these data were obtained before the filament was moved 80 mm downstream).

The decrease in emission intensity of the argon lines appears to be consistent with the observed divergence of the ion plume: Namely, because the observation region has a finite height, the fraction of the plume which is imaged onto the detector decreases as the plume expands. Also, the decrease in emission intensity in Fig. 4 follows the same pattern as the decrease in electron current at plasma potential obtained with a Langmuir probe (see Fig. 4 of Ref. [14]).

Figure 5 shows similar results for radial scans of the plume, performed at two axial locations. Again, the spatial variation of ion and neutral signals is essentially identical. From Fig. 5, we estimate that the plume diameters (enclosing 95 percent of the ion flux) are 25 mm at x = 0 mm and 44 mm at x = 60 mm, respectively. These values imply a 9 degree half-angle for the plume divergence. This value is larger than the calculated value of 5.5 degrees (see Fig. 13 in Section 7). As is pointed out in Section 7, this is probably due to beam broadening as a result of elastic and/or inelastic scattering off the fairly high density neutral gas in the facility.

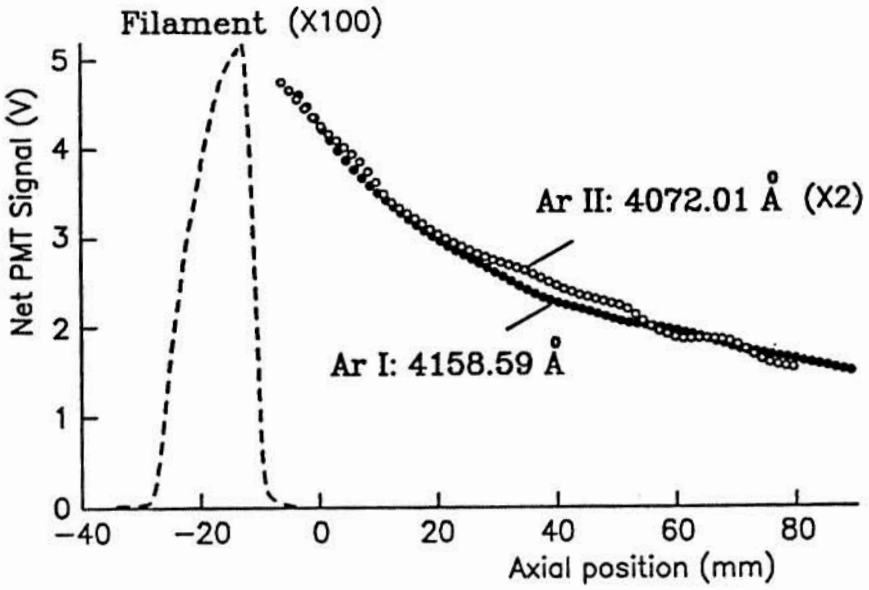

Figure 4: *Axial variation of emission intensity for an argon neutral line (Ar I), an argon ion line (Ar II), and the filament background. The coiled filament is located at about z = -15 mm; the accelerator grid is located at about z = -25 mm. Data taken with V_B = 500 V.*

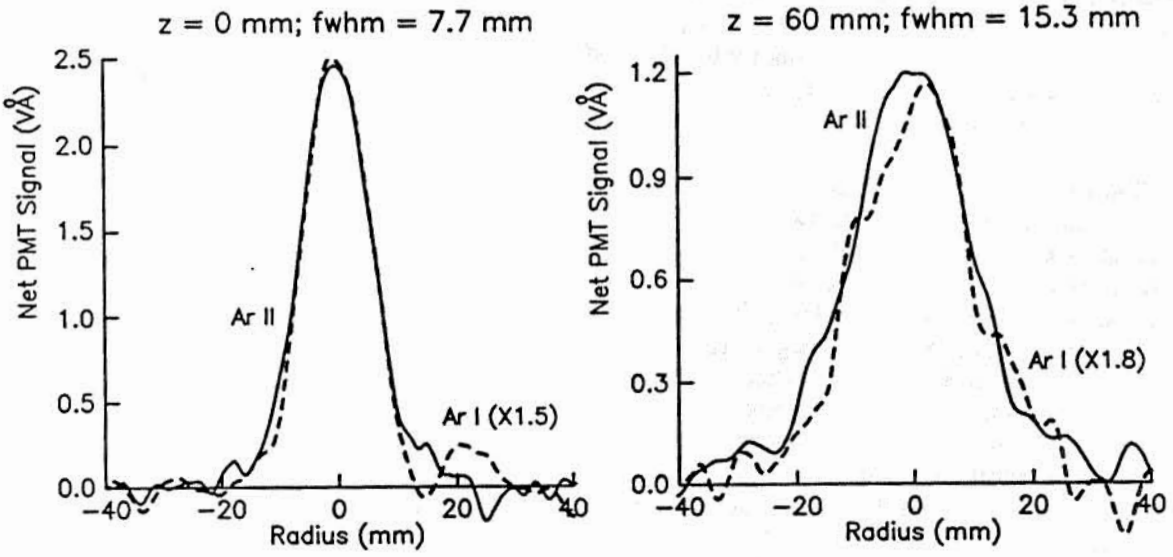

Figure 5: *Radial variation of emission intensity at two axial positions, for the same conditions as in Fig. 4.*

Table I: *Beam-plasma interactions which we consider in this study. Asterisks indicate excited states.*

$$(1) \quad Ar^{+}_{fast} + e \rightarrow (Ar^{+}_{fast})^{*} + e$$

$$(2) \quad Ar^{0}_{slow} + e \rightarrow (Ar^{0}_{slow})^{*} + e$$

$$(3) \quad Ar^{0}_{slow} + e \rightarrow (Ar^{+}_{slow})^{*} + 2e$$

$$(4) \quad Ar^{+}_{fast} + e \rightarrow (Ar^{++}_{fast})^{*} + 2e$$

$$(5) \quad Ar^{+}_{fast} + Ar^{0}_{slow} \rightarrow \begin{cases} Ar^{0}_{fast} \\ (Ar^{0}_{fast})^{*} \end{cases} + \begin{cases} Ar^{+}_{slow} \\ (Ar^{+}_{slow})^{*} \end{cases}$$

$$(6) \quad Ar^{+}_{fast} + Ar^{0}_{slow} \rightarrow \begin{cases} Ar^{+}_{fast}(\vartheta) \\ (Ar^{+}_{fast})^{*}(\vartheta) \end{cases} + \begin{cases} Ar^{0}_{\text{“slow”}}(90^{0} - \vartheta) \\ (Ar^{0}_{\text{“slow”}})^{*}(90^{0} - \vartheta) \end{cases}$$

4. Identification of interaction mechanisms

In the absence of beam-plasma interactions, the only heavy species in the plume would be fast beam ions (ions with kinetic energies of at least several hundred electron volts) and slow neutral atoms (atoms with no more than several electron volts of kinetic energy). Both would either be in the ground state or a metastable state, and no emission would be observed. To account for the observed plume emissions it is necessary to identify the different excitation mechanisms.

In Table I we list the interactions which we believe to be most important [19]. The first two are: (1) electron impact of beam ions; and (2) electron impact of slow neutrals. The second pair is: (3) ionization of slow neutrals by electron impact; and (4) production of doubly-charged ions by electron impact of singly charged beam ions. We did not find any evidence of doubly charged ions in the broad survey spectra. However, no concentrated effort was made to identify such doubly charged ions, so we cannot rule out their existence. Neither of the reactions (1) through (4) are accompanied by significant momentum transfer to the heavy collision partner. Thus the velocity vectors of the ions and neutrals are unchanged during the excitation process.

The remaining two processes in Table I involve interactions between fast beam ions and slow neutrals. They are: (5) charge-exchange collisions; and (6) elastic or inelastic scattering. Figure 6 illustrates the two processes. In the first one (5) a fast beam ion exchanges an electronic charge with a slow neutral atom, leaving behind a slow ion and a fast neutral atom. Little momentum transfer takes place, so the resulting fast neutral has essentially the same vector velocity as the original beam ion. The charge-exchange ion picks up a small (but superthermal) velocity, perpendicular to the path of the beam ion.

In the other process (6) from Fig. 6, both the beam ion and the thermal neutral maintain their identities (ion and

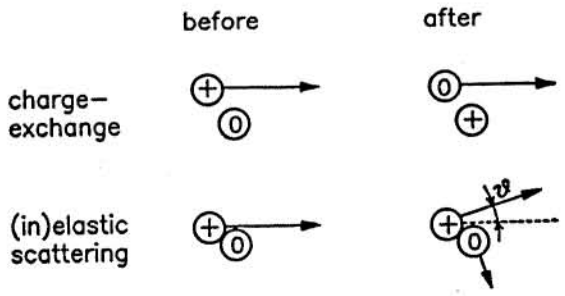

Figure 6: *Schematic representation of charge-exchange and (in)elastic scattering processes between fast beam ions and slow neutral atoms. In an inelastic collision, one or both of the scattering partners are left in an excited state after the collision.*

neutral, respectively). However, depending on the impact parameter of the collision, both are scattered. For small impact parameters, the scattering angles can be large. Thus the velocity vector of the incident beam ion can be modified significantly (both in magnitude and direction), and the thermal neutral atom can pick up a significant velocity. Conservation of momentum implies that the velocity vectors after the collision are orthogonal.

Both processes (5) and (6) may give rise to plume emission directly. This occurs when one of the scattering partners is left in an excited state after the collision. This is the case in an *in*elastic collision. Alternatively, it is possible that excitation of the scattering product does not occur until *after* the collision, namely upon electron impact of the elastically scattered product by one of the reactions (1) through (4) from Table I. We cannot distinguish between these two scenarios on the basis of the present set of experiments.

However, the above description of the relevant beam-plasma interactions invites several conjectures which may be verified experimentally. These concern the dependence of emission intensities on neutral densities; the interpretation of the emission lineshape as a measure of the velocity distribution of the emitting species through the Doppler effect; and the broadening of the plume with increasing neutral density. These conjectures, with supporting experimental data, are discussed in Sections 5, 6, and 7.

5. Dependence of emission on neutral density

Among the six interactions identified in Table I, processes (1) and (4) stand out as the only ones which should be independent of the neutral density in the plume. By contrast, the rates of all other processes in Table I should be linearly proportional to the neutral density. This leads to the following conjectures:

Conjecture 1: The emission intensity from neutral atoms should be proportional to the neutral density and extrapolate to zero in the limit of zero neutral density. This is because all neutral emissions involve either the neutral atom itself, or a neutral collision partner in the case of a charge-exchange reaction.

Conjecture 2: The emission intensity from singly ionized ions should vary linearly with neutral density. However, unlike for neutral emissions, emissions from ions should contain a signal component which is independent of the neutral density, namely that which is associated with electron excitation of beam ions.

Conjecture 3: The emission intensity from doubly charged ions should be independent of the neutral density, because only beam ions and electrons are involved.

To test the first two conjectures, a series of experiments was performed in which the spectrometer was scanned repeatedly across a particular spectral line. The neutral density in the plume was varied either by flowing gas into the chamber through the bypass valve, or by increasing the flow rate through the source. However, all electrical parameters of the ion source were kept constant. In particular, the beam current was kept constant. Emission intensities were calculated by curve-fitting the recorded spectral lines with a gaussian model function. This procedure was found to be quite adequate to calculate the area under the spectral line, even though the fit did not always approximate the data very well.

Figures 7 and 8 show some of the results. In Figure 7, the emission signal of the argon neutral line at 4159 Å is plotted as a function of chamber pressure for different flow rates. Figure 8 shows similar data for the argon ion line at 4880 Å. To test conjectures 1 and 2, bilinear curve fits were performed to the data from Figs. 7 and 8, according to:

$$S_{PMT} = A + B \times P + C \times \dot{m}^* \qquad (1)$$

where S_{PMT} is the emission signal, P is the chamber pressure, and $\dot{m}^*$ is the net neutral flow through the source. This net flow is the actual flow rate through the source, corrected for the flow equivalent of the ionized fraction of the plume (1 sccm of flow per 64 mA of current for argon).

The solid lines in Figs. 7 and 8 represent the results of the bilinear curve fits. They are found to approximate the data quite well, thereby verifying the conjecture of a linear dependence of emission intensity on neutral density. The dashed lines represent the extrapolated pressure dependence in the limit of zero net neutral flow though the source. This limit corresponds to 100 percent propellant utilization efficiency, and cannot be achieved experimentally with our source.

To distinguish between conjectures 1 and 2, we need to identify the signal contribution in the limit of zero neutral density. This limit is given by the intercept of the dashed curves with the vertical axes in Figs. 7 and 8, given by the parameter A from Eq. (1). In Fig. 7, this intercept is given by $A = 0.064 \pm 0.051$, where the standard deviation is calculated from the bilinear curve fit. That is, the neutral signal extrapolated to zero neutral density is negligible, in agreement with conjecture 1.

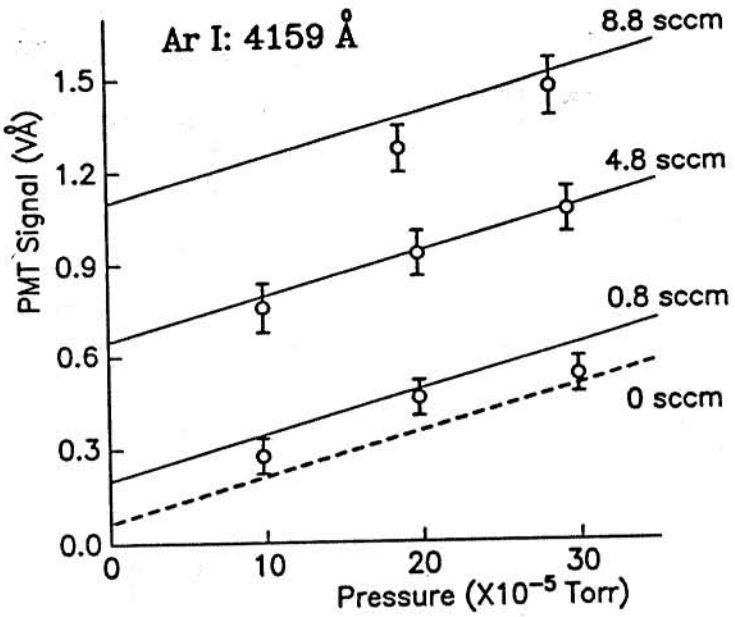

Figure 7: *Dependence of emission intensity on chamber pressure and net neutral flow rate (in sccm) for the argon neutral line at 4159 Å. Experimental conditions were as follows: V_D = 50 V; V_B = 900 V; V_A = -500 V; J_B = 80 mA; α = 71.4°. Solid and dashed lines represent the results of a bilinear curve fit.*

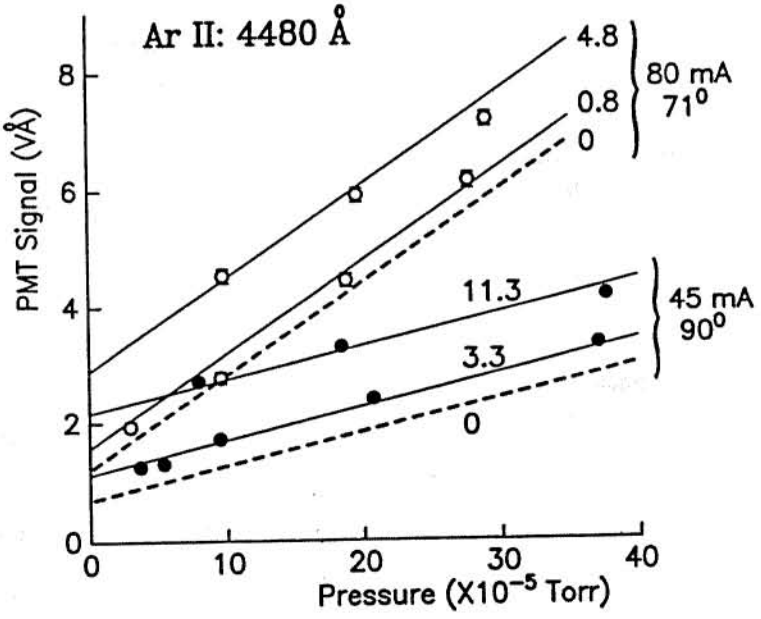

Figure 8: *As Fig. 7, for the argon ion line at 4880 Å. Conditions were V_D = 50 V; V_B = 900 V; V_A = -500 V; J_B = 80 mA; α = 71.4° for upper set of data, and V_D = 50 V; V_B = 500 V; V_A = -500 V; J_B = 45 mA; α = 90° for the other.*

On the other hand, both sets of data in Fig. 8 yield a non-vanishing contribution for the emission of an ion line in the limit of zero neutral density, namely A = 1.20 ± 0.20 for the set of data taken with a beam current of 80 mA, and A = 0.683 ± 0.095 for a beam current of 45 mA. Both of these values are statistically significant at the level of six standard deviations. Thus, they are convincing proof that part of the emission signal is due to electron excitation of the ion plume, as stated in conjecture 2.

So far, no systematic effort has been made to identify emissions from doubly charged ions. Thus conjecture 3 can neither be verified nor rebutted at this point.

In principle, it should be possible to establish, in similar fashion, the dependence of the emission intensity on the ion flux. We have found that, indeed, the strength of the emission signals increases with beam current. However, it is not clear a priori whether this dependence should be linear. In particular, we expect that the electron density in the plume is strongly correlated with the ion density, so as to maintain a charge-neutral beam. Thus it is conceivable that even processes which do not involve beam ions (electron excitation or ionization of slow neutrals) should show a dependence on beam current. Similarly, electron excitation of beam ions might depend nonlinearly on the beam current as a result of the coupling between positive and negative charge. For these and other reasons, a systematic study of the dependence of emission intensity on beam current is rather complicated, and we have not undertaken such a study here.

6. Lineshape measurements

In order to clarify the role of the different contributions to the observed emission lines, we performed detailed measurements of the emission lineshapes. One of the primary mechanisms to determine lineshape is Doppler broadening. Namely, let the non-Doppler shifted wavelength of an emission line be given by λ_0. If the emitting atom has a velocity component v_l along the observation direction, the observed emission wavelength is Doppler shifted by an amount $\Delta\lambda_D$, given by

$$\Delta\lambda_D = \lambda_0 \times (v_l / c), \qquad (2)$$

where c is the speed of light. The shift is toward lower wavelength for an atom moving toward the detector. This Doppler shift can be substantial for the beam ions excited by electron impact [process (1) from Table I] and for charge-exchange neutrals [process (5) from Table I], which continue traveling at beam velocities. For a beam voltage V_B, a discharge voltage V_D, and an observation angle α (either 90^0 or 71.4^0 in our experiments), the projected velocity for a beam atom moving along the centerline of the source is given by:

$$v_l = [(2e/m)\times(V_D+V_B)]^{1/2} \times \cos\alpha, \qquad (3)$$

where e/m is the charge-to-mass ratio of the beam ion. As an example, for V_D = 900 V, V_B = 50 V, $\alpha = 71.4^0$ and λ_0 = 8115 Å (a strong argon neutral line), Eqs.(2) and (3) yield a negative shift of 0.58 Å. Given the spectrometer resolution of 0.1 Å or better, it should be straightforward to resolve this shift. This leads to the following conjecture:

Conjecture 4: Through the Doppler shift, it should be possible to separate the emissions from fast beam ions and fast charge-exchange neutrals on the one hand, and of slow ions and neutrals on the other.

To test this conjecture, we have measured a number of emission lineshapes for both ion and neutral lines. Typical results are shown in Figs. 9 and 10. Figure 9 shows the recorded emission lineshape for the conditions of the example above (circles are experimental data; the curve fits are discussed in Section 7). These data were obtained with 25 micron slits on the spectrometer. The instrument line width at this setting is 0.10 Å at full-width-half-maximum (fwhm).

The lineshape in Figure 9 clearly consists of two peaks, separated exactly by the calculated Doppler shift of -0.58 Å. Thus, the left component of the line can be identified unambiguously as the charge-exchange neutral contribution. By inference, the right component must be due to excited neutrals, excited either by inelastic scattering with the ion beam [process (6) in Table I] or by electron impact of slow neutrals [process (2) of Table I]. Neutral atoms excited in either process are predominantly slow-moving, so that they are centered at zero Doppler shift. In fact, the origin of the Doppler shift scale in Figure 9 is chosen such that it coincides exactly with the center of the right emission peak.

Measurements were also performed on the same spectral line for a different beam voltage (V_B = 500 V), and on a different neutral line (7635 Å, V_B = 900 V). In both cases, the separation of the two peaks was consistent with the Doppler shifts calculated from Eqs.(2) and (3). Further discussion of the observed lineshapes is given in Section 7. We conclude that conjecture 4 has been verified for neutral lines.

For ion lines, the situation is slightly different. This is clear from Fig. 10 which shows the lineshape of the argon ion line at 4880 Å. This measurement was performed with the same instrument resolution as the data from Fig. 9. However, because of the lower emission wavelength, the

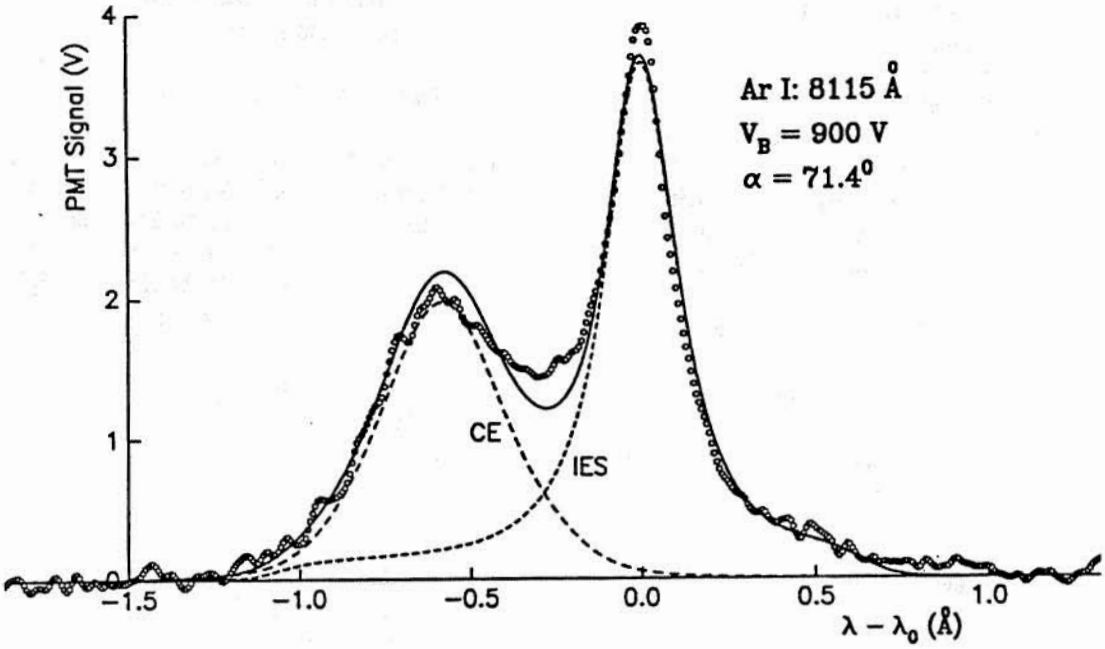

Figure 9: *Observed emission lineshape of the 8115 Å argon neutral line, at an observation angle of 71.4°. Circles represent experimental data. Dashed lines are based on the model calculations discussed in Section 7. The solid line is the sum of the two dashed lines.*

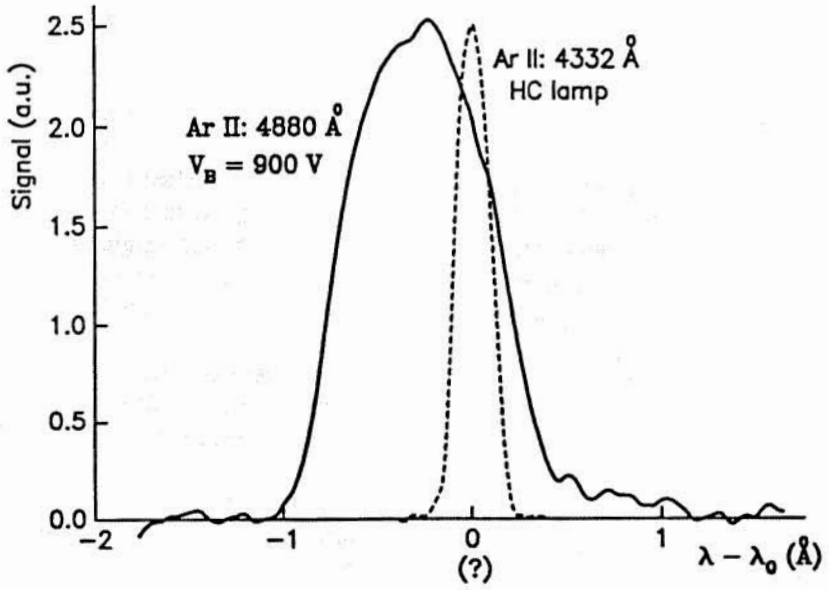

Figure 10: *Observed emission lineshape of the 4880 Å argon ion line, for the same conditions as in Figure 9. The origin of the Doppler shift scale has been fixed at an arbitrary position. For comparison, the scan of an argon ion line from a hollow cathode lamp is shown also.*

Doppler shift between the fast and slow components is smaller than in Fig. 9. Primarily as a result of this, we believe, the double peak structure of the emission line is obscured, so that conjecture 4 has not been verified for an ion line.

Unfortunately, no strong argon ion emission occurs at significantly larger wavelengths. To resolve this situation, we intend to repeat the measurements at a larger observation angle α. Also we plan to check if sufficient signal can be collected on one of the "reddest" argon ion lines tabulated in Ref. [18], around 6800 Å.

Because no clear two-peaked structure is evident in the ion lineshape from Fig. 10, we were unable to locate the origin of the Doppler shift scale unambiguously. Even without being able to resolve the double-peaked structure for the ion line, this situation could be improved by recording a simultaneous reference signal. For example, the emission from a low power argon discharge could be used for this purpose. As an example, a typical scan of such a spectral line from a hollow cathode lamp is shown in Fig. 10 along with the emission lineshape from the ion plume.

Even in the absence of a good absolute wavelength calibration, an attempt was made to measure the shift of the center of the argon ion line from Fig. 10 as a function of the beam voltage. Figure 11 displays the measured line positions along with the theoretical prediction from Eqs.(2) and (3). The precision of the wavelength determination was limited to about 0.015 Å, as determined by the procedure for setting the marker signal on the spectrometer. Also, the two series of data did not reproduce well. Nevertheless, it is evident from Fig. 11 that the center of the line (arbitrarily defined as the point of gravity of the lineshape) shifts in agreement with the predictions from Eqs.(2) and (3).

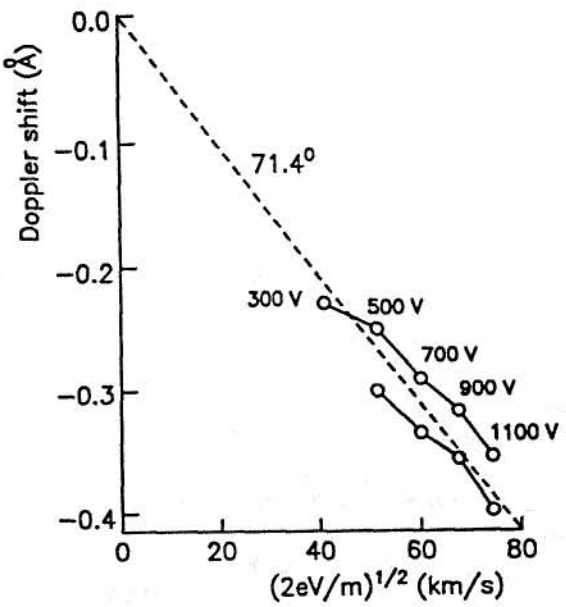

Figure 11: *Measured (circles) versus calculated line positions (dashed) of the argon ion line from Fig. 10 for beam voltages of 300, 500, 700, 900, and 1100 V; J_B = 40 mA; $\dot{m}$ = 4 sccm. The vertical scale has been fixed arbitrarily.*

7. Further analysis of the lineshapes

Of course, one important factor which determines the width of the measured spectral lines is the spectrometer resolution. Even at best, this resolution is insufficient to allow a determination of the true width of the emission signals from slow neutrals and slow ions. On the other hand, the widths of the emission lines associated with emissions from beam ions and from charge-exchange neutrals should reflect the distribution of plume angles for the respective species. These distributions of plume angles are primarily determined by the ion optics of the ion source. However, especially at high background densities, additional beam broadening may result due to elastic and/or inelastic scattering of beam ions, as is illustrated in the lower diagram of Fig. 6.

An intermediate case is provided by neutrals which have been scattered through a large angle as a result of a collision with a beam ion at small impact parameter. Such neutrals may have a substantial velocity after the collision, giving rise to broadening of the slow peak of a neutral emission line. In this case, the associated lineshape is determined in large part by the differential scattering cross-section for the elastic or inelastic collision.

The above arguments can be formulated in terms of specific conjectures for each of the components of the ion and neutral lines. We refrain from this because the analysis to support these conjectures is as yet incomplete. However, we discuss several results which elucidate the principles involved.

Figure 12 shows the measured line widths of the argon ion lines which form the basis for the data from Fig. 11. It is evident that the observed line widths increase dramatically as the beam energy is increased. This is consistent with the interpretation that the line width of the fast component of the emission lineshape is determined in large part by the divergence of the plume. The dotted lines in Fig. 12 correspond to points of equal plume divergence as indicated. It follows that the plume divergence increases slightly as the beam energy is increased.

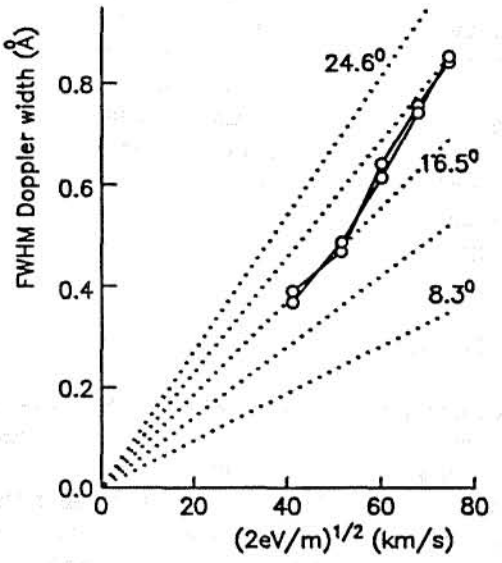

Figure 12: *Measured line widths, corresponding to the data from Fig. 11. The dotted lines indicate points of equal beam divergence, measured as the enclosed angle at full-width half-maximum of the beam profile.*

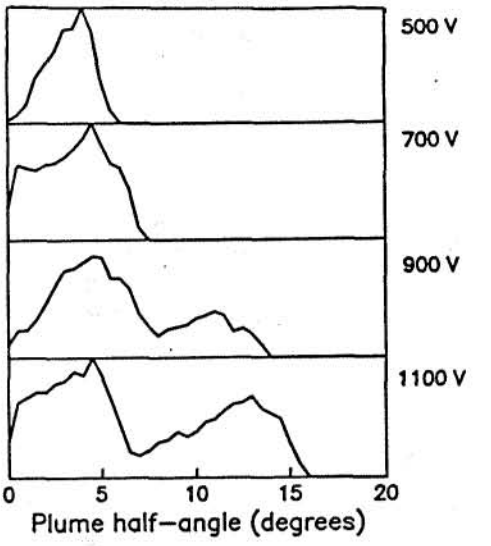

Figure 13: *Calculated distribution of beam angles corresponding to the conditions from Figs. 11 and 12 for values of beam voltage as indicated. No elastic or inelastic scattering was taken into account.*

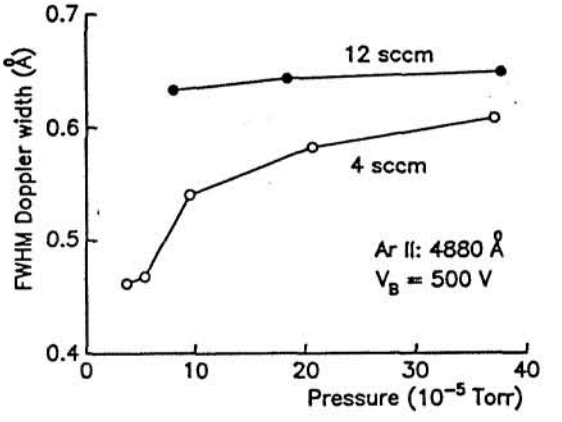

Figure 14: *Measured line width of the argon ion line at 4880 Å as a function of chamber pressure and total mass flow rate through the source.*

This effect was verified by a numerical simulation of the ion optics of the 3 cm source, using our previously developed code. Figure 13 shows the resulting distribution of plume half-angles (defined as the angle of a given beam ion to the axis of the source), for the same conditions as in the experiment. Specifically, Fig. 13 shows that, indeed, the distribution of plume half-angles widens as the beam voltage is increased (we do not have an explanation for the bimodal distributions of plume angles for $V_B \geq 900$ V). The measured divergences in Fig. 12 are actually somewhat larger than the calculated values. This can be explained by the combination of instrument broadening and beam broadening as a result of elastic scattering.

Figure 14 shows the effect of beam broadening as a result of elastic or inelastic scattering explicitly. Namely, as the chamber pressure is raised by flowing additional gas into the chamber through the bypass valve, the width of the 4880 Å ion line increases significantly. For a high neutral flow rate through the source (the curve marked 12 sccm in Fig. 14), the effect is even more serious, and even larger line widths result.

Finally, we have performed a series of calculations to reproduce the measured emission lineshapes explicitly. The calculations are similar to those in Ref. [20]. They are rather involved, and we discuss them here only briefly. The calculated distribution of plume angles from Fig. 13 is used as a starting point. By integration over the polar angles ϑ_i and φ_i from Fig. 15, the projections v_i of the beam ions (or charge-exchange neutrals) along the observation direction are calculated. The resulting distribution of projected velocities is then converted to a distribution of Doppler shifts, and convolved with the instrument profile. As an example, the fast component of the neutral line from Fig. 9 was modeled.

The resulting curve is shown in Fig. 9 as a dashed curve, marked 'CE' to indicate that it corresponds to charge-exchange neutrals. The agreement between the

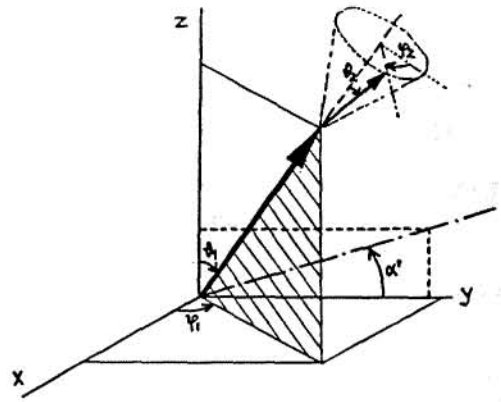

Figure 15: *Polar scattering diagram used to compute the projections of beam and scattered ion velocities onto the observation direction, taken to lie in the yz-plane at an angle* $\alpha' = 90^0 - \alpha$ *to the y-axis.*

theoretical curve and the experimental data is quite impressive for the left side of the fast peak, where the contribution from the slow peak is small. This agreement is even more remarkable when considering that only one adjustable parameter was needed to match the theoretical curve to the data, namely the amplitude of the peak.

We have also attempted to account for the "left-over" part of the lineshape from Fig. 9, given by the difference of the experimental data and the dashed curve marked 'CE'. This "slow" peak, centered at zero Doppler shift, consists of slow neutrals excited by electron impact, and of neutrals scattered by elastic and/or inelastic collisions with beam ions. To model the latter process, it was necessary to perform an integration over a second set of polar angles (ϑ_2 and φ_2 in Fig. 15) for each beam angle, to account for the scattering process. Furthermore, it was necessary to assume a particular form for the differential scattering cross-section for the corresponding process. As is illustrated by the dashed curve marked 'IES' in Fig. 9, it was indeed possible to model the peak at zero Doppler shift in this way, including the relatively broad wings which result from large-angle scattering at small-impact parameters. Although the results are still rather tentative, they indicate that it may be possible to model the emission lineshapes accurately even for such complicated interactions.

8. Discussion and conclusions

It is generally assumed that the measurement of velocity distributions of plasma species through exploitation of the Doppler effect is only possible in experiments in which a narrowband laser is used as the wavelength-selective element. For example, we have previously shown how the technique of laser induced fluorescence can be used to measure exit velocities in arcjet plumes [21-22].

Here we have shown that, actually, high-resolution emission spectroscopy *can* be used to characterize the beam-plasma interactions in the plume from an ion source. Much information can be gained from the analysis of the emission lineshapes of both neutral and ion lines. Specifically, because of their large plume velocities, it is possible to measure the Doppler shifts of fast beam ions and fast charge-exchange neutrals directly. Also, it is possible to distinguish these emissions from those arising from electron impact of slow neutrals, elastically and/or inelastically scattered neutrals, and slow charge-exchange ions.

We propose that the new technique be employed to study various processes in the downstream plasma region of ion thruster engines. Specifically, we have shown that it is possible to identify charge-exchange collisions between beam ions and slow neutral atoms, as well as electron impact excitation of beam ions. Indirect evidence for electron impact ionization of background neutral atoms has been found as well.

Other diagnostic applications of this spectroscopic technique can be envisioned as well. Among these are: estimation of electron temperatures in the plume by analyzing the ratio of ion-to-neutral emission intensities [13]; measurement of beam broadening as a result of the interaction of the plume with the background gas; and further use of the optical measurements to verify the numerical codes. Finally, the spectroscopic measurements serve as a valuable stepping stone toward more sophisticated experiments based on the technique of laser induced fluorescence.

Acknowledgements

This work was supported by Boeing Defense & Space Group, Seattle, Washington, and by NASA grant NAGW-1195. We are especially indebted to N. Wright for his technical support.

References

[1] X. Peng, W. M. Ruyten, and D. Keefer, "Plasma particle simulation of electrostatic ion thrusters," AIAA paper 90-2647, 21st International Electric Propulsion Conference, Orlando, Florida, July 18-20, 1990.

[2] X. Peng, W. M. Ruyten, V. J. Friedly, and D. Keefer, "Plasma particle simulation of electrostatic ion thrusters," Proceedings of the 2nd Annual Technical Symposium, CSTAR, Tullahoma, Tennessee, November 1-2, 1990, pp. 73-78.

[3] X. Peng, W. M. Ruyten, and D. Keefer, "Monte Carlo simulation of ion-neutral charge exchange collisions and grid erosion in an ion thruster," AIAA paper 91-0607, 29th Aerospace Sciences Meeting, Reno, Nevada, January 7-10, 1991.

[4] X. Peng, W. M. Ruyten, and D. Keefer, "Particle simulation of grid erosion in ion thrusters," AIAA paper 91-2120, 27th Joint Propulsion Conference, Sacramento, California, June 24-26, 1991.

[5] X. Peng, W. M. Ruyten, and D. Keefer, "Three-dimensional particle simulation of grid erosion in ion thrusters," Paper 91-119, 22nd International Electric Propulsion Conference, Viareggio, Italy, October 14-17, 1991.

[6] X. Peng, D. Keefer, and W. M. Ruyten, "Plasma particle simulation of electrostatic ion thrusters," *AIAA Journal of Propulsion and Power*, Vol. 8, No. 2, March-April 1992, pp. 361-366.

[7] X. Peng, W. M. Ruyten, and D. Keefer, "Ion thruster modeling," Proceedings of the 3rd Annual Technical Symposium, CSTAR, Tullahoma, Tennessee, January 14-15, 1992, pp. 91-97.

[8] X. Peng, W. M. Ruyten, and D. Keefer, "Further study of the effect of the downstream plasma condition on accelerator grid erosion in an ion thruster," paper AIAA-92-3829, 28th AIAA Joint Propulsion Conference, Nashville, Tennessee, July 6-8, 1992.

[9] J. Monheiser and P. Wilbur, "An experimental study of impingement-ion-production mechanisms," paper AIAA-92-3826, Nashville, Tennessee, July 6-8, 1992.

[10] N. Hershkowitz, "How Langmuir probes work," in "Plasma Diagnostics, Volume 1," edited by O. Auciello and D. L. Flamm, Academic Press, Boston, 1989, pp. 113-183.

[11] P. M. Chung, L. Talbot, and K. J. Touryan, "Electrical probes in stationary and flowing plasmas: theory and applications," Springer-Verlag, New York, 1975.

[12] Y. Hayakawa, K. Miyazaki, and S. Kitamura, "Measurements of electron energy distributions in an ion thruster," *J. Propulsion and Power*, Vol. 8, No. 1, pp. 118-126, 1992.

[13] T. I. Cox, et al., "The use of Langmuir probes and optical emission spectroscopy to measure electron energy distribution functions in RF-generated argon plasmas," *J. Phys. D: Appl. Phys.*, Vol. 20, No. 7, pp. 820-831, 1987.

[14] D. Keefer, W. Ruyten, V. Friedly, and J. Meserole, "Ion propulsion: experimental work," CSTAR Quarterly Report, January 1, 1992 - March 31, 1992, pp. 34-39.

[15] P. M. Latham, A. R. Martin, and M. T. Cresdee, "Optical emission spectrum of the UK-10 ion thruster operating on xenon," paper 88-112, Proceedings of the 20th International Electric Propulsion Conference, Garmisch-Partenkirchen, October 1988, pp. 627-633.

[16] R. Goldstein and K. M. Monagan, "Optical properties of mercury ion thruster exhaust plumes; significance for candidate SEP science instruments," paper AIAA-75-362, New Orleans, Louisiana, March 1975.

[17] W. M. Ruyten and D. Keefer, "Arcjet plume diagnostics," these proceedings.

[18] Wiese, Smith, and Miles, "Atomic Transition Probabilities: Sodium through Calcium," National Bureau of Standards, publication No. 22.

[19] J. B. Hasted, "Physics of atomic collisions," Butterworks, London, 1964.

[20] F. J. Morgan, A. Marcuzzi, and C. H. Dugan, "Shapes of optical emission lines from atoms excited by fast ion impact: I. calculated results," *Can. J. Phys.*, Vol. 52, 2525-2533, 1975.

[21] W. M. Ruyten and D. Keefer, "Laser fluorescence velocimetry of an arcjet exhaust plume," Paper 91-093, 22nd International Electric Propulsion Conference, Viareggio, Italy, October 14-17, 1991; also to appear in *AIAA J.*

[22] W. M. Ruyten and D. Keefer, "Characterization of electric thruster plumes using multiplexed laser induced fluorescence measurements," AIAA paper 92-2965, 23rd AIAA Plasma Dynamics and Lasers Conference, Nashville, Tennessee, July 6-8, 1992.